Supplementary information

Unveiling Excitation-Independent Visible Photoluminescence of SnO_2 Nanodots for Precise Latent Fingerprint Identification Powered by Artificial Intelligence

Subhamay Pramanik[1,*], Jayashree Karmakar[2], Sumit Mukherjee[3], Sk Irsad Ali[4], Shiv Prakash Verma[1], Anshika Bansal[1], Sukanta Pal[5], Riju Karmakar[6], Atis Chandra Mandal[4], Probodh K. Kuiri[3]

[1] *School of Nano Science and Technology, Indian Institute of Technology Kharagpur, Kharagpur, 721302, India*
[2] *Department of Biological Sciences and Engineering, Lowa State University, Lowa-50011, USA*
[3] *Department of Physics, Sidho-Kanho-Birsha University, Purulia, 721104, India*
[4] *Department of Physics, The University of Burdwan, Bardhaman, 713104, India*
[5] *Department of Chemistry, Sidho-Kanho-Birsha University, Purulia, 721104, India*
[6] *Department of Chemical Engineering, Indian Institute of Technology Delhi, Delhi, 110016, India*

X-ray photoelectron spectroscopy analysis:

The XPS survey spectra of all three samples viz., SnO_2/P, SnO_2/10h and SnO_2/20h has been shown in figure S1, all three spectra show characteristics peaks corresponding to the Sn and O_2. The Sn 3d peak, located around 487 eV, corresponds to the Sn(IV) oxidation state [1], while the O1s peak, typically found around 530 eV, indicates the presence of oxygen in the lattice structure [2]. No other peaks corresponding to any impurity has been observed ensure the purity of the samples even after mechanical milling [3]. The detail analysis of the O1s is provided in the manuscript section of figure 4(e-f). Here figure S1(d) shows the oxygen vacancy density as a function of milling time which ensure the gradual increase of oxygen vacancy as the mechanical milling time increases.

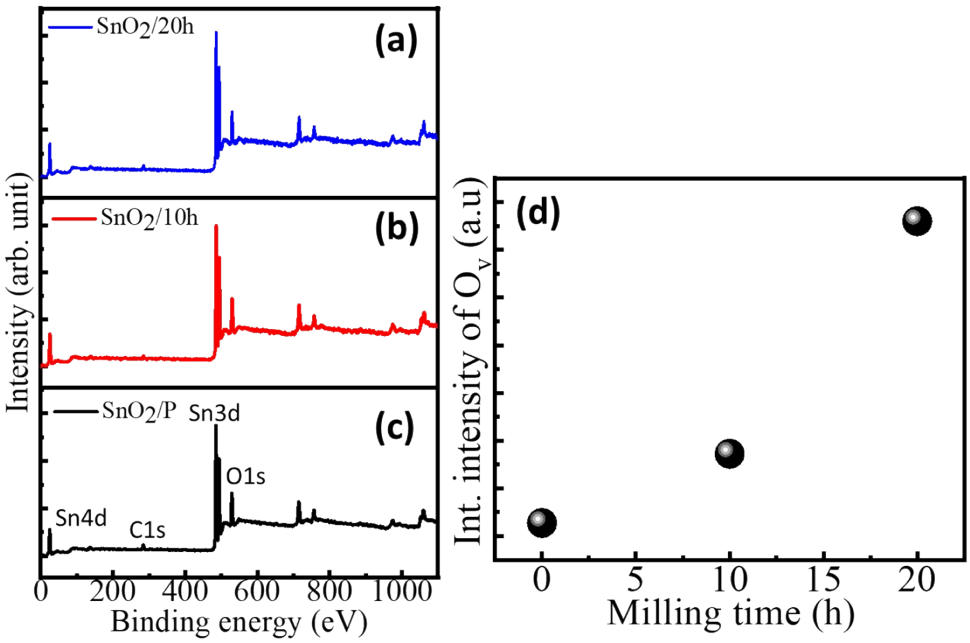

Figure S1: XPS survey spectra of all three samples (a) SnO_2/P, (b) SnO_2/10h and (c) SnO_2/20h respectively. Oxygen vacancy density as a function of milling time is in (d).

EDS and elemental mapping:

The EDS spectrum of SnO_2/20h is shown in figure S2(a). The EDS and elemental mapping of the SnO_2/20h sample reveal the distribution tin (Sn) and oxygen (O), within the material. The EDS spectrum provides the elemental composition, confirming the presence of tin and oxygen as the main constituents. Elemental mapping in figure S2(b-d), displayed as color-coded overlays, shows how tin and oxygen are distributed across the sample surface.

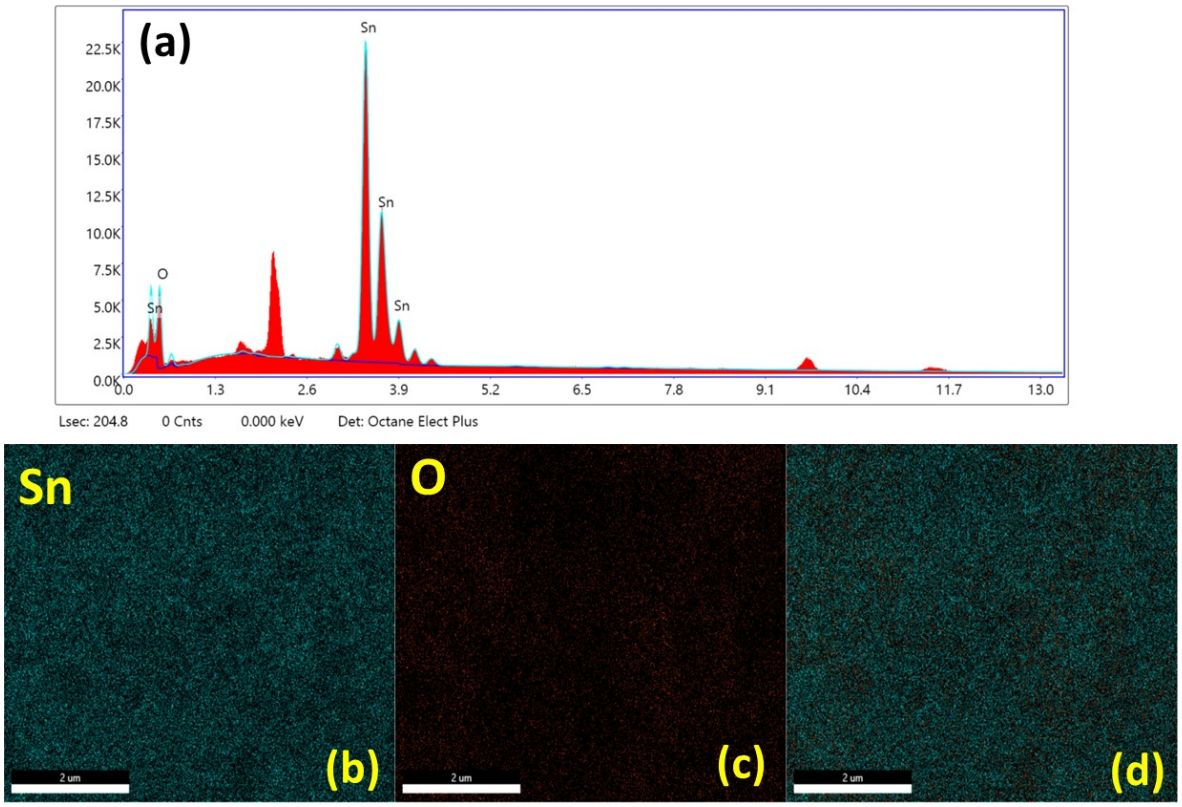

Figure S2: The EDS spectrum of the SnO_2/20h in (a). The elemental mapping of the same one in (b) Sn (c) O and (d) SnO_2 respectively.

Photoluminescence analysis:

Figure S3(a) shows Gaussian fitted PL spectrum of SnO_2/20h sample for the excitation wavelength of 250 nm. The fitted peak position is located at UV and visible region, the UV peak is located 380-400 nm, the visible emission peaks with centre is 425 nm, 450 nm, 490 nm, 515 nm and 435 nm respectively.

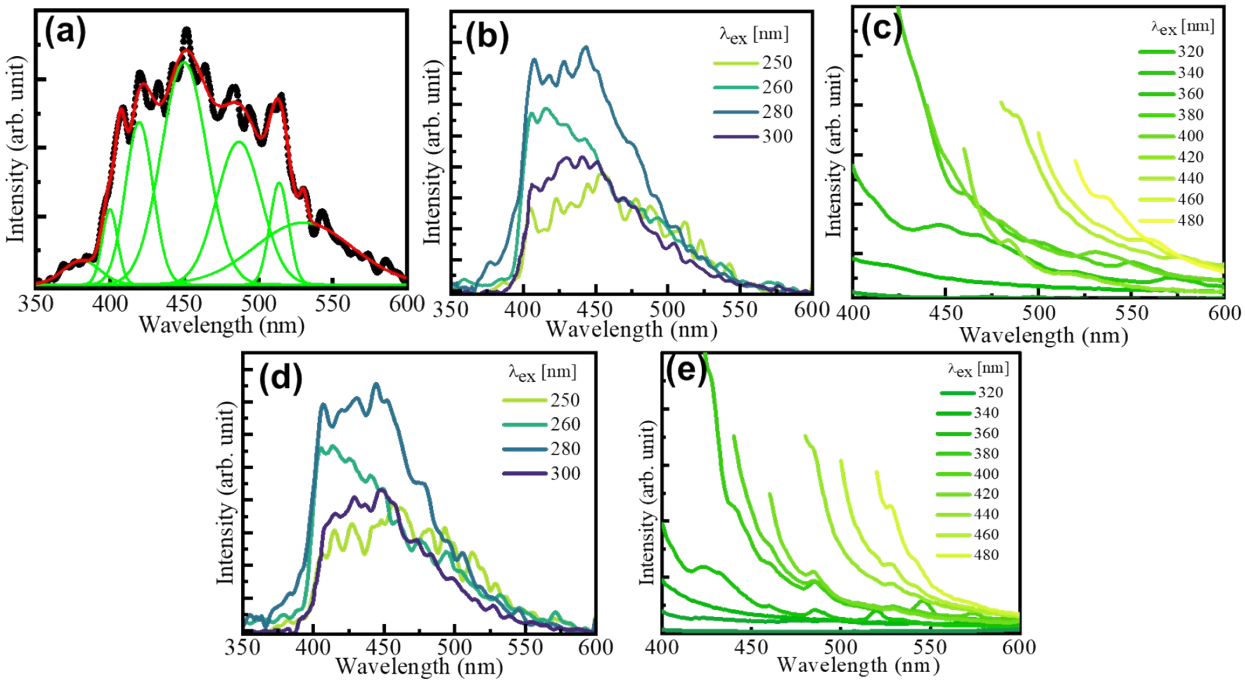

Figure S3: Fitted PL spectrum of SnO_2/20h for the excitation of 250 nm (a), shows several emission centres, the detail of these emission centres discussed in the manuscript section. Normalised PL spectra of SnO_2/P and SnO_2/10h for different excitation wavelength viz above (b, d) and below (c, e) the bandgap energies respectively.

LFP analysis:

The LFPs on different substrates were collected using the following method: The finger was first cleansed with a soap solution and then dried with a hot air dryer. Following that, the thumb finger was lightly rubbed over the tip of the nose to check for oily attachment, and then the substrates listed above were lightly pressed. Finally, the fresh LFPs were lightly dusted with SnO_2/20h sample and images were taken under 254 nm UV excitation.

The human fingerprint contains many minute details like ridge dots, bifurcations, ridge islands, enclosures, etc. which are called Galton de tails [4]. Figure S4 (a) shows the control image of the LFP taken using “ink fingerprinting” technique. The LFP on a hard plastic substrate after dusting SnO_2 NDs and under the illumination of UV 254 nm is shown in figure S4(b). The magnified view of some specific marked region is shown in Fig. S4 (c), one can clearly observe all the minute details of the fingerprint numbering from 1 to 6. The minute details of the fingerprint satisfied the characteristics of fingerprint identifications, hence luminescence SnO_2 NDs can be used as a potential candidate for LFP detection. Figure S4 (d) shows the line profile shown in Fig. S4(b), marked as the red line. One can clearly differentiate the ridge and furrows of the fingerprint in the line intensity profile curve. Such prominent variation of the pixel profile

value over the fingerprint ensures that SnO_2 NDs can effectively recognize LFPs. The substrate dependent LFPs under the excitation of 254 nm UV light is shown in figure S4 (e-h) respectively.

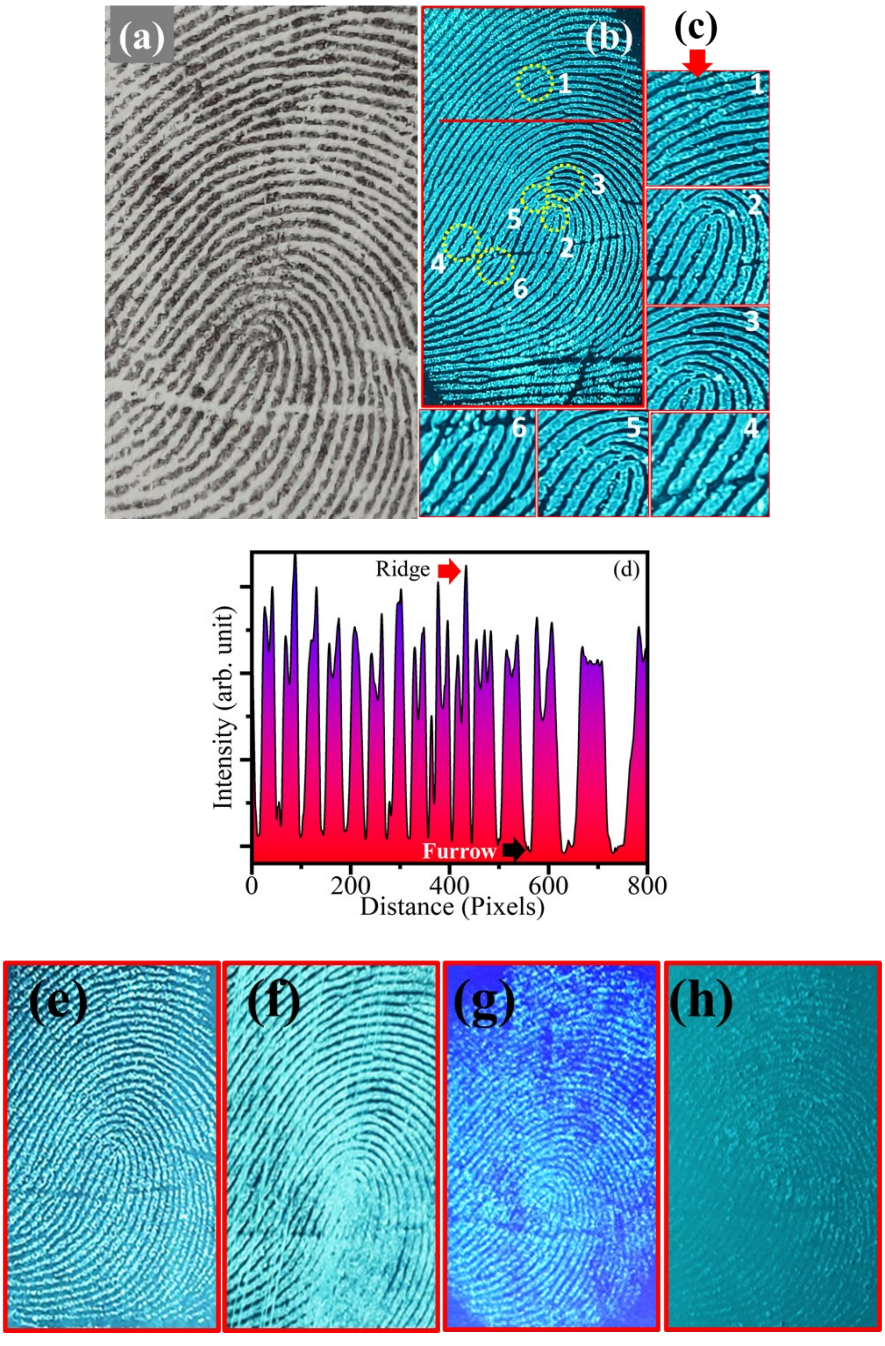

Figure S4: Control LFP of the subject taking using "Ink Printing" techniques. LFP on plastic substrate after dusting SnO_2/20h sample of a 30-year-old person under 254 nm. The minutes details of the LFP shown in fig S3 (c) 1–6, (1) ridge ending (2) core (3) bifurcation (4) ridge dot (5) crossed bifurcation (6) lake. The intensity line profile of the red marked line in (figure S3(b)) in (d), One can clearly differentiate the ridge and furrows of the fingerprint in the line intensity profile curve. Such prominent variation of the pixel profile value over the fingerprint ensures that SnO_2 NDs can effectively recognize LFPs from different objects. Substrate

dependent LFPs under the excitation of 254 nm UV light viz., (e) glass (f) aluminium sheet (g) polypyrrole sheet (ppy) and (h) white marble respectively.

References:

[1] R. Samanta, M. Kempasiddaiah, R. K. Trivedi, B. Chakraborty, and S. Barman, *ACS Appl. Energy Mater*. 2024, 7, 5359−5370.

[2] S. Acharyya, P. K. Guha, *Appl. Surf. Sci*, (2024), 655, 159640.

[3] S. Pramanik, S. Mondal, A. C. Mandal, S. Mukherjee, S. Das, T. Ghosh, R. Nath, M. Ghosh, P. K. Kuiri, *J. of Alloys. Compd.* (2020), 849, 156684.

[4] L.K. Bharat, G.S.R. Raju, J.S. Yu, *Sci. Rep.* (2017), 7, 11571,